Fall 2014

Fe(II)-catalyzed recrystallization of hematite

Maria Rose Helgeson
University of Iowa

FE(II)-CATALYZED

RECRYSTALLIZATION OF HEMATITE

by

Maria Helgeson

A thesis submitted in partial fulfillment of the requirements for the
Master of Science degree in Civil and Environmental Engineering
in the Graduate College of
The University of Iowa

December 2014

Thesis Supervisor: Professor Michelle M. Scherer

Graduate College
The University of Iowa
Iowa City, Iowa

CERTIFICATE OF APPROVAL

MASTER'S THESIS

This is to certify that the Master's thesis of

Maria Helgeson

has been approved by the Examining Committee for
the thesis requirement for the Master of Science
degree in Civil and Environmental Engineering at the December 2014
graduation.

Thesis Committee:

Michelle M. Scherer, Thesis Supervisor

David Cwiertny

Timothy Mattes

To my parents, thank you for your constant love and support.

ABSTRACT

Iron oxides are abundant throughout the earth's crust. In nature, Fe(III) at the surface of Fe oxides can be reduced to Fe(II) by dissimilatory iron reducing bacteria (DIRB), causing the oxides to come into contact with aqueous Fe(II). It is known that some Fe oxides undergo Fe atom exchange in the presence of aqueous Fe(II) as a result of electron transfer from sorbed Fe(II) to the oxides; this transfer results in oxidative growth and reductive dissolution. Fe atom exchange has been observed in ferrihydrite, lepidocrocite, goethite, and magnetite. Since Fe oxides can contain trace metal substituents as well as micronutrients, Fe atom exchange has implications for the fate and transport of several elements and compounds in the environment.

Hematite (α-Fe_2O_3) is one of the most common Fe oxides, and is of particular interest because of its relative stability. This characteristic makes hematite a good candidate for use as a photoanode in photoelectrochemical (PEC) cells, which are used to produce clean energy in the form of hydrogen gas (H_2) via a water splitting reaction. It has also been proposed that hematite could serve as an indicator of historical environmental changes, since it is sensitive to changes in temperature and humidity. However, if hematite is to be used as an environmental indicator or incorporated into PEC cells, a thorough understanding of its surface chemistry will be essential.

Previous research has not directly observed Fe atom exchange between Fe(III) in hematite and aqueous Fe(II). However, the release of trace metals from hematite in the presence of Fe(II) implies that this exchange does occur. In this work, enriched isotope tracer experiments

were used to demonstrate Fe atom exchange between Fe(III) in hematite and aqueous Fe(II). The effects of particle size, pH, and the concentration of aqueous Fe(II) on the extent of exchange were also investigated.

PUBLIC ABSTRACT

Hematite (α-Fe_2O_3) is a common, naturally occurring iron oxide, found throughout the earth's crust and atmosphere. Hematite is of interest to the scientific community because it is able to catalyze a reaction that produces hydrogen gas (H_2), which is a form of clean energy. The composition of hematite in nature is also used to make inferences about conditions on early earth's surface. Hematite is useful for clean energy production and as an environmental indicator partly because of its apparent stability. However, some evidence suggests that hematite might not be as stable as previously thought.

Many iron oxides undergo Fe atom exchange when they come into contact with aqueous Fe(II), as often occurs in nature. This atom exchange can result in elements and nutrients being taken up or released from the iron oxides as they recrystallize. Although atom exchange has not been directly observed in hematite, it has been demonstrated that trace metals are released from hematite in the presence of aqueous Fe(II), implying that exchange may be occurring. Here, we directly observe Fe atom exchange between hematite and aqueous Fe(II). This work provides information concerning the surface chemistry of hematite and has important implications for clean energy production and the environment.

TABLE OF CONTENTS

LIST OF FIGURES

CHAPTER I INTRODUCTION

Iron oxides are naturally abundant minerals, found ubiquitously throughout the earth's crust and atmosphere. Iron oxides in nature are impacted by the activity of dissimilatory iron reducing bacteria (DIRB). DIRB are capable of reducing Fe(III) to Fe(II) at iron oxide surfaces, thereby impacting the reactivity of iron oxides with respect to nutrients, metals, and organics (Bose et al., 2009). DIRB can also reduce humic substances, which are then capable of reducing Fe(III) in Fe oxides (Diepenbrock et al., 2014). Reduction of Fe(III) in Fe oxides by DIRB or other reduced compounds causes a flux of Fe(II) at Fe oxide surfaces, leading to Fe(II) sorption onto the oxides (Larese-Casanova et al., 2012).

Sorption of Fe(II) to Fe oxides often results in electron transfer from aqueous Fe(II) to Fe(III) in oxides. Transfer of electrons from Fe(II) to Fe(III) in oxides has been demonstrated for goethite, hematite, and ferrihydrite (Boland et al., 2014, Williams & Scherer, 2004, Larese-Casanova & Scherer, 2007, Cwiertny et al., 2008). Injection of electrons can lead to Fe oxide recrystallization; ferrihydrite has been shown to transform into lepidocrocite, goethite, and magnetite as a result of electron transfer from Fe(II) (Boland et al., 2014). Electron transfer from Fe(II) to goethite is not inhibited by Al-substitution or by the presence of PO_4^{2-}, CO_3^{2-}, or SiO_4^{2-} (Latta et al., 2012), suggesting that it is likely to occur under natural conditions.

Iron oxides including ferrihydrite, lepidocrocite, goethite, and magnetite can undergo Fe atom exchange with aqueous Fe(II) following sorption and electron transfer (Pedersen et al., 2005, Jones et al., 2009, Gorski et al., 2012, Handler et al., 2009). High levels of exchange have been observed in goethite (≈90%) (Handler et al., 2014) with less observed for magnetite (10%) (Handler et al., 2014). Iron atom exchange has also been observed for the Fe-containing sulfate minerals jarosite and schwertmannite (Jones et al., 2009). Enriched isotope tracer experiments

are used to determine the extent of atom exchange between aqueous Fe(II) and Fe(III) in Fe oxides.

The mechanism behind Fe atom exchange between aqueous Fe(II) and Fe(III) in Fe oxides is thought to depend on oxidative growth coupled with reductive dissolution (Figure 1) (Frierdich et al., 2011, Yanina & Rosso, 2008). Oxidative growth occurs when Fe(II) sorbs and donates an electron to Fe(III) in the mineral. That electron can then be passed from Fe atom to Fe atom within the Fe oxide. Reductive dissolution occurs when an injected electron reduces Fe(III) on the oxide surface to Fe(II), causing it to dissolve into the aqueous phase.

Fe atom exchange also occurs, although sometimes to a lesser extent, in Fe oxides containing organic matter and trace metal substituents. Substitution with aluminum and trace elements appears to inhibit atom exchange in goethite (Latta et al, 2012, Frierdich et al., 2014), and high concentrations of silicon and natural organic matter were observed to inhibit exchange in several Fe oxides (Jones et al., 2009). However, the extent of exchange in goethite was not significantly affected by the presence of phosphates (Latta et al., 2012), and exchange in magnetite was not inhibited by cobalt substitution (Gorski et al., 2012).

Fe(II)-catalyzed recrystallization of Fe oxides impacts the fate of certain environmental contaminants that may be incorporated into the oxides, including trace metals and organics. These pollutants may be taken up from or released into groundwater as a result of Fe oxide recrystallization (Frierdich & Catalano, 2012, Cwiertny et al., 2008, Boland et al., 2014). Many Fe oxides in nature are biogenic in origin, formed as a result of Fe(II) oxidation by bacteria (Piepenbrock et al., 2014); these biogenic Fe oxides often contain organic matter. Additionally, the uptake and release of heavy metals such as arsenic and uranium is influenced by interactions

between Fe(II) and Fe(III) in oxides (Boland et al., 2014, Handler et al., 2009, Kappler et al., 2011).

Of the Fe oxides, hematite (α-Fe_2O_3) is of particular interest because of its potential for clean energy production. Hematite is one of the most common Fe oxides, and exists in nature in several forms including rhombohedra, hexagonal plates, and ellipsoids (Echigo et al., 2013). Hematite appears to function well as a photoanode in photoelectrochemical (PEC) cells, which produce hydrogen (H_2) in the presence of sunlight through a water-splitting reaction (Bora et al., 2013):

$$\text{Anodic reaction: } 2\ H_2O \rightarrow O_2 + 4\ H^+$$

$$\text{Cathodic reaction: } 4\ H^+ \rightarrow 2\ H_2$$

The ubiquity of hematite in nature makes it an attractive low-cost option for PEC cell construction. Hematite has also recently garnered attention because its ubiquity, relative stability, and sensitivity to temperature and humidity changes make it a good indicator of historical environmental changes (Guo et al., 2013). As a result, the reactivity of hematite is of interest in the field of environmental health. However, if hematite is to be adopted for large-scale use in PEC cells or used as an environmental indicator, an understanding of the redox chemistry of this Fe oxide will be essential.

Previous research has not observed atom exchange between aqueous Fe(II) and Fe(III) in hematite. Under conditions that led to significant levels of atom exchange in ferrihydrite, lepidocrocite, and goethite, no exchange was observed for hematite (Pedersen et al., 2005). However, it has been shown that aqueous Fe(II) can sorb to hematite and reduce Fe(III) in a hematite crystal (Larese-Casanova & Scherer, 2007, Yanina & Rosso, 2008). Furthermore, electrons can be passed from Fe atom to Fe atom within hematite crystals, establishing a bulk

flow of electrons and resulting in oxidative growth at one face of the crystal coupled with reductive dissolution at another face. This Fe(II)-catalyzed redox activity suggests that Fe atom exchange between aqueous Fe(II) and Fe(III) in hematite likely does occur.

In this study, an enriched isotope tracer approach was used to investigate Fe atom exchange between Fe(III) in hematite and aqueous Fe(II). Two particle sizes of hematite were synthesized and characterized. Exchange reactions were then carried out with hematite of each particle size. The extent of exchange was also tracked as a function of reaction pH and initial Fe(II) concentration.

CHAPTER II HEMATITE SYNTHESIS AND CHARACTERIZATION

Synthesis Methods

Hematite was synthesized as described by Pedersen et al. and following Method 2 in Cornell & Schwertmann's Iron Oxides in the Laboratory. Following synthesis, all particles were washed by centrifugation, dried in an oven at 70^{o}C, and sieved. Phase purity was analyzed by X-ray diffraction (XRD) and no crystalline phases other than hematite were identified. Specific surface area and particle size for each hematite material was determined by N_2 adsorption BET analysis, and scanning electron microscopy (SEM) and transmission electron microscopy (TEM).

Hydrochloric acid dissolution of hematite solids was carried out in 4M HCl at an initial solids loading of 1 g/L. Dissolution reactions were mixed end over end. Samples (1 mL) were collected and filtered (0.22 mm, nylon) into clean 1 mL microcentrifuge tubes.

Discussion

Hematite was synthesized according to the method described by Pedersen et al. (2005) so that a comparison could be made between the isotope exchange results seen here and those observed by Pedersen. BET analysis of the hematite synthesized as described by Pedersen showed a specific surface area of 27 m^2g^{-1}. Hematite was also synthesized by following Method 2 in Iron Oxides in the Laboratory (Schwertmann & Cornell, 2000) so that isotope exchange could be tracked in two different hematite particle sizes. The hematite synthesized by following Method 2 had a BET-measured specific surface area of 54 m^2g^{-1}. SEM images shown in Figure 2 confirmed that hematite particles synthesized following Schwertmann & Cornell's Method 2 (hereafter referred to as 54 m^2g^{-1} hematite) had a smaller diameter than particles synthesized following the method described by Pedersen et al. (hereafter referred to as 27 m^2g^{-1} hematite), as shown in Table 1.

Table 1: Synthesis Methods and Hematite Characterization Data
Synthesis method details as well as BET-measured specific surface area (SSA) and average diameter determined from SEM images for each type of hematite synthesized.

Synthesis Method	BET-measured SSA (m^2g^{-1})	Average Diameter (nm)	N (Particles Counted)
3.75 mM HCl heated to 98° C for 7 days following addition of $FeCl_3$ to final concentration of 0.02 M (Pedersen et al., 2005)	27	68 ± 9	50
0.2 M $Fe(ClO_4)_3$ solution heated at 98° C for 7 days (Schwertmann & Cornell, 2000)	54	58 ± 7	50

XRD analysis of both types of hematite before isotope exchange reactions showed that no iron oxide other than hematite was present in significant amounts (Figure 3). A Mössbauer spectrum of 54 m^2g^{-1} hematite at 140°K (Figure 4) showed a sextet with weakly ferromagnetic parameters (center shift = 0.46 mm/s; quadrupole splitting = -0.10 mm/s and hyperfine splitting of 52.5) and anti-ferromagnetic parameters (center shift = 0.47 mm/s; quadrupole splitting = 0.21 mm/s and hyperfine splitting of 53.4) similar to those previously observed for hematite (Larese-Casanova & Scherer, 2007).

Fe(II) sorption was quantified as a function of pH and aqueous Fe(II) concentration for both 27 and 54 m^2g^{-1} hematite (Figure 5). Both particle sizes showed similar increases in Fe(II) sorption as pH increased from 3 to 9. Sorption started to occur around pH 5.5, with the greatest increase in sorption occurring between pH 5.5 and 8.5. As a result, isotope exchange experiments were carried out at pH values ranging from 5.5 to 8.0. These values were consistent with earlier work done by Larese-Casanova and Scherer (2007), which shows an increase in Fe(II) sorption by hematite as pH increases between 6.6 and 8.1. Our work showed a total sorption of more than 200 μmol of Fe(II) per gram of 54 m^2g^{-1} hematite at pH 7.5, while earlier work by Larese-Casanova and Scherer (2007) showed a total sorption of approximately 90 μmol of Fe(II) per gram of 30 m^2g^{-1} hematite at pH 7.4.

As expected, more sorption of Fe(II) was observed on the larger surface area hematite (54 m^2g^{-1}) compared to the smaller surface area hematite (27 m^2g^{-1}) at pH 7.5. For both types of hematite, the greatest increase in Fe(II) sorption occurred as initial Fe(II) concentration increased from 0 to 1.0 mM. Based on the pH edge and sorption isotherm data, isotope exchange experiments were carried out using initial Fe(II) concentrations ranging from 0.5 to 4.0 mM with pH values ranging from 5.5 to 8.0 where measurable sorption occurred.

CHAPTER III Fe(II)-CATALYZED RECRYSTALLIZATION

Introduction

Enriched isotope tracer experiments were carried out with the intent of observing whether Fe atom exchange would occur between hematite and aqueous Fe(II). Although Fe atom exchange was not observed between hematite and aqueous Fe(II) in previous research, some experiments suggest that this exchange does occur. Here, we investigated Fe atom exchange using two different hematite particle sizes. The effect of varying pH and Fe(II) concentration was also examined.

Methods

Isotope exchange reactions used natural isotopic abundance hematite and ^{57}Fe(II). All exchange experiments were carried out in an anoxic glovebox (93% N_2, 7% H_2) with a Pd catalyst to remove trace oxygen. A solution of 0.1 M ^{57}Fe(II) was prepared by dissolving ^{57}Fe(0) in HCl in a sealed serum bottle for 24 hours. Isotopic exchange reactors contained 2 g/L hematite, 10 mL of 25 mM HEPES buffer (4-(2-hydroxyethyl)piperazine-1-ethanesulfonic acid, *N*-(2-hydroxyethyl)piperazine-*N'*-(2-ethanesulfonic acid)) for pH 7.0, 7.5 and 8.0 reactors or 10 mL of 25 mM MES buffer (2-(*N*-morpholino)ethanesulfonic acid) for pH 5.5 and 6.5 reactors, as well as 25 mM KBr as a background electrolyte. The pH was adjusted to 5.5, 6.5, 7.0, 7.5 or 8.0 using 1 M KOH. Aliquots of ^{57}Fe(II) were added to bring the initial Fe(II) concentration to 0.5, 1.0, 2.0, or 4.0 mM. Duplicates were constructed for each set of reaction conditions.

Reactors were left on a rotator in the dark; duplicates were sacrificed at time points ranging from one hour to 60 days. Zero time point reactors containing no hematite were also constructed. A 1 mL aliquot was taken from each sacrificed reactor and centrifuged inside the glovebox at ~6200x g for 1.5 minutes. The supernatant was discarded and the pellet was

resuspended in 0.4 M HCl for 10 minutes. The suspension was centrifuged a second time and the supernatant was filtered (0.22 mm, nylon) into a clean 2 mL microcentrifuge tube and saved for analysis. The pellet was dissolved in 4 M HCl at 70^0 C prior to ICP-MS analysis. The remainder of the original reactor suspension was filtered and acidified to a final concentration of 0.4 M HCl.

Fe isotopic analyses were carried out using a Thermo Fisher Scientific X Series II Quadrupole ICP-mass spectrometer in collision cell mode with a glass concentric nebulizer and a HEPA filtered autosampler. The percent of Fe exchange in hematite was calculated as discussed in our prior work (Handler et al., 2014):

Equation 1: Percent Fe Exchange

$$\% \text{ Fe Exchange} = \frac{N_{aq} \times (\delta^{i}_{aq} - \delta^{t}_{aq}) \times 100}{N^{T}_{Hem} \times (\delta^{t}_{aq} - \delta^{i}_{Hem})}$$

Where N_{aq} represents the total initial moles of Fe(II) in the system, N^{T}_{Hem} represents the total initial moles of Fe(III) in hematite, δ^{i}_{aq} is the initial fraction of aqueous ^{57}Fe, δ^{i}_{Hem} is the initial fraction of ^{57}Fe(III) in hematite, and δ^{t}_{aq} is the fraction of aqueous ^{57}Fe at a time point.

Exchange between Aqueous Fe(II) and Hematite

Iron isotope exchange experiments were carried out between natural abundance hematite and ^{57}Fe-enriched Fe(II). ICP-MS analysis was used to determine the fraction of each isotope in aqueous samples. In a typical reaction, a fast decrease in aqueous ^{57}Fe was observed, accompanied by a corresponding increase in ^{56}Fe and a slight increase in ^{54}Fe (Figure 6). The changes in isotope fractions occur quickly, with a significant change in the first two days followed by a much slower change for the next 28 days. The decrease in ^{57}Fe and increase in

^{56}Fe and ^{54}Fe in the aqueous phase indicate that Fe atoms are exchanging between the aqueous phase and hematite solids.

In all reactions, the fractions of ^{57}Fe in each of the three reaction phases, solid, aqueous, and sorbed, approached the mass balance over time (Figure 7). This equilibration of the fraction of ^{57}Fe in each phase again indicates that isotope exchange is occurring between the three. Most exchange occurs quickly, with each phase approaching a steady-state fraction of ^{57}Fe by three days. It was also observed that in all reactions, the fraction of ^{57}Fe in the sorbed phase was essentially equal to the fraction of ^{57}Fe in the aqueous phase at all times.

Atom Exchange as a Function of Particle Size

Pedersen et al. (2005) observed fast release of ^{55}Fe-labelled iron oxides including ferrihydrite, lepidocrocite, and goethite when the oxides were exposed to aqueous Fe(II). However, their research did not show significant release of ^{55}Fe from hematite. They concluded that hematite was unaffected by the presence of Fe(II) due to its high stability. Our research sought to reconcile the data collected by Pedersen et al. with other sets of data that imply Fe isotope exchange between hematite and an aqueous phase based on observations of metal release from hematite in the presence of Fe(II) (Frierdich, 2012).

Using the change in isotope fractions we can estimate the fraction of Fe atoms that have exchanged with the aqueous phase using Equation 1. We observed isotope exchange in both types of hematite synthesized, with Fe isotope exchange in 54 m^2g^{-1} hematite about five times as high as exchange in 27 m^2g^{-1} hematite by 30 days (2.0 g/L solids loading, 1.0 mM Fe(II), pH 7.0) (Figure 8). The higher amount of exchange observed in 54 m^2g^{-1} hematite was likely due to its relatively higher exposed surface area, which allows for more sorption of Fe(II) to the hematite.

While 27 m^2g^{-1} hematite seemed to have reached its maximum amount of exchange by 14 days, 54 m^2g^{-1} hematite appeared to still be exchanging at 30 days.

After 30 days, 24% Fe exchange was observed in 54 m^2g^{-1} hematite, whereas only 5% exchange was observed in 27 m^2g^{-1} hematite. At pH 7.5 and with an initial concentration of 1 mM Fe(II), 54 m^2g^{-1} hematite sorbed 228 μmol of Fe(II) per gram of hematite, whereas 27 m^2g^{-1} hematite sorbed 127 μmol of Fe(II) per gram of hematite (Figure 5b). Therefore, 54 m^2g^{-1} hematite sorbed twice as much Fe(II) as 27 m^2g^{-1} hematite at circumneutral pH and in the presence of 1 mM Fe(II), but underwent five times as much Fe atom exchange.

Characterization After Exchange

XRD analysis of both types of hematite after 30-day isotope exchange reactions showed no conversion of hematite to other iron oxides (Figure 3). Samples of both 54 m^2g^{-1} and 27 m^2g^{-1} before and after isotope exchange reactions were dissolved in 4M HCl at a solids loading of 1 g/L (Figure 9). Unreacted hematite controls were dry powders. Given that 4 mg of hematite were used in each dissolution reaction, a theoretical maximum concentration of 1.25 mM Fe(III) was calculated. After 3.5 hours, a dissolved Fe(III) concentration of 0.83 mM was measured in the reactor containing unreacted 54 m^2g^{-1} hematite, whereas a concentration of only 0.39 mM was measured in the reactor containing 54 m^2g^{-1} hematite after a 30-day exchange reaction. At 3.5 hours, reacted 27 m^2g^{-1} hematite had also only dissolved about half as much as unreacted 27 m^2g^{-1} hematite. The reduced rate of dissolution observed for hematite that has undergone isotope exchange reactions could indicate that hematite particles underwent aggregation during exchange reactions.

Atom Exchange as a Function of pH

Due to the fact that more Fe exchange was observed in 54 m^2g^{-1} hematite than in 27 m^2g^{-1} hematite at circumneutral pH, 54 m^2g^{-1} hematite was used for variable pH and initial concentration of Fe(II) reactions. The effect of pH of Fe isotope exchange was investigated through reactions carried out at pH values of 5.5, 6.5, 7.0, 7.5, and 8.0. The results showed that the amount of exchange seen by 80 days increased as pH increased from 5.5 to 7.5 (Figure 10). The amount of exchange seen at pH 7.5 and pH 8.0 at 80 days was the same within error.

The trend in Fe isotope exchange with increasing pH parallels the trend in Fe(II) sorption as pH increases over the same range (Figure 5). At pH 7.5, 33% Fe isotope exchange was seen in 54 m^2g^{-1} hematite by 33 days, while at pH 5.5 only 8% exchange had occurred by 31 days. The same type of hematite sorbed 48 μmol of Fe(II) per gram of hematite at pH 5.4 and 258 μmol per gram at pH 7.3. In this case, sorption of Fe(II) increased by a factor of about five while Fe isotope exchange increased by a factor of four over the same pH range.

A similar trend of increase in Fe isotope exchange with increasing pH has been observed in goethite, where approximately 90% exchange was seen after 30 days at pH 7.5, and less than 15% was observed over the same time span at pH 5.0 (Handler et al., 2014). In goethite, as here, lower exchange at the more acidic pH correlated with much lower sorption of Fe(II) at that pH.

Atom Exchange as a Function of Fe(II) Concentration

For reactions using 54 m^2g^{-1} hematite at varying initial concentrations of Fe(II), Fe exchange decreased as the initial concentration of Fe(II) increased from 1.0 to 4.0 mM (Figure 11). These results may seem counterintuitive, especially since Fe(II) sorption to hematite increases with increasing Fe(II) concentration (Figure 5). However, this increase in sorption with increasing Fe(II) concentration levels off at an Fe(II) concentration of approximately 1.0 mM. It

is likely that at a solids loading of 2 g/L, the hematite surface becomes saturated with sorbed Fe(II) above concentrations of 1.0 mM. The literature reports that the average maximum surface site density of hematite is 2.5 sites per nm^2 (Jeon et al., 2004). Assuming one Fe(II) atom can sorb per site, and using the BET-measured specific surface area of 54 m^2g^{-1}, this means that theoretically this hematite can sorb 225 μmol of Fe(II) per gram before becoming saturated with Fe(II). The sorption isotherm created for 54 m^2g^{-1} hematite shows that sorption does indeed level off at a maximum of approximately 225 μmol of Fe(II) per gram of hematite (Figure 5). This sorption saturation point could explain why Fe exchange does not increase as initial Fe(II) concentration increases beyond 1 mM. Furthermore, saturation of the hematite surface with sorbed Fe(II) may block the remaining aqueous Fe(II) from the hematite, meaning that a smaller portion of the total pool of initial Fe(II) comes into contact with the hematite surface. This could be the cause of the decrease in percent exchange of Fe as the initial concentration of Fe(II) increases.

The Pedersen iron oxide exchange experiments were carried out at pH 6.5 with a solids loading of 0.0399 mg/L and Fe(II) concentrations ranging from 0 to 1.0 mM. With an initial concentration of 0.6 mM Fe(II), Pedersen et al. observed that there was no measurable release of ^{55}Fe from hematite after 26 days. This seems consistent with our observations. At pH 7.5 and with an initial Fe(II) concentration of 1.0 mM and solids loading of 2 g/L, hematite synthesized as specified by Pedersen et al. exchanged up to 4% Fe with the aqueous phase after 30 days. At a lower pH and with the low solids loading and Fe(II) concentration used by Pedersen, we would expect to see negligible Fe exchange between hematite and the aqueous phase based on our results. Thus, hematite does undergo the isotope exchange Pedersen et al. observed in

ferrihydrite, lepidocrocite, and goethite, but only at a higher pH, solids loading or Fe(II) concentration than used by Pedersen et al.

CHAPTER IV SUMMARY AND ENGINEERING SIGNIFICANCE

Previous research on atom exchange between Fe(III) in hematite and aqueous Fe(II) did not directly demonstrate exchange between the two pools of Fe (Pedersen et al., 2005). However, coupled oxidative growth and reductive dissolution, along with the release of trace metals under reducing conditions, implied that Fe exchange could occur (Frierdich & Catalano, 2012, Frierdich et al., 2011). Under the conditions used here, up to ≈40% exchange was observed between Fe(III) in hematite and aqueous Fe(II). The extent of exchange was greater in particles with a higher specific surface area. Exchange also increased as pH increased from 5.5 to 7.5, but decreased as the initial concentration of aqueous Fe(II) increased.

Evidence of Fe exchange between Fe(III) in hematite and aqueous Fe(II) has important implications for environmental trace element fate and transport. Fe exchange in Fe oxides leads to cycling of incorporated trace elements and contaminants through the oxides (Frierdich & Catalano, 2012, Frierdich et al., 2011). This cycling affects contaminants in groundwater and the availability of micronutrients to microorganisms. Previous research has shown that the rate of contaminant and micronutrient release is controlled by the rate of Fe oxide recrystallization (Frierdich et al., 2011). The transfer of electrons from atom to atom within Fe oxides can also affect the redox state of redox-active trace elements. Additionally, the composition of iron oxides in geologic strata is often used to make extrapolations about element and micronutrient availability on early earth's surface. The knowledge that Fe atom exchange occurs and affects trace element fate could affect interpretations of the composition of prehistoric Fe oxides.

Future work on this subject could further investigate Fe atom exchange between Fe(III) in hematite and aqueous Fe(II) by examining whether the extent of exchange is affected by the

presence of minerals and compounds found in natural environments, such as trace metals and phosphates.

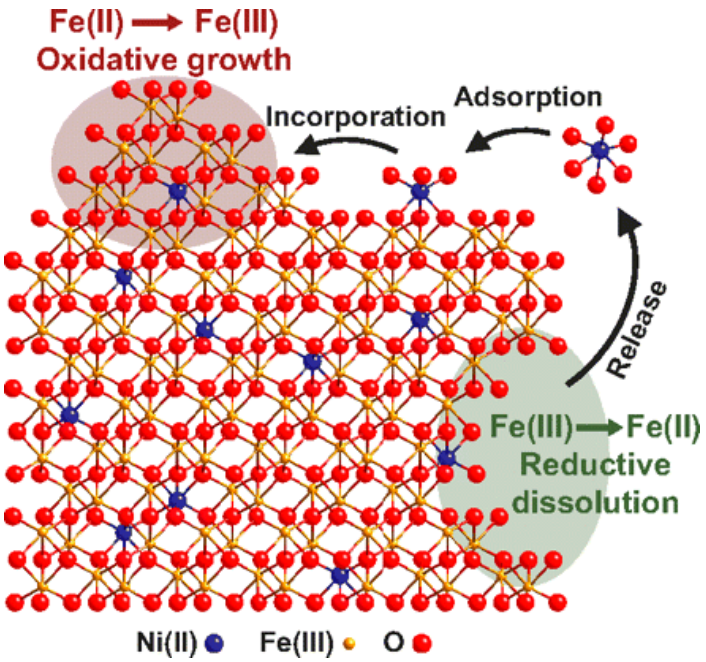

Figure 1: Diagram of Fe atom exchange

Illustration of Fe atom exchange between aqueous Fe(II) and Fe(III) in an Fe oxide via oxidative growth coupled with reductive dissolution (Frierdich et al., 2011).

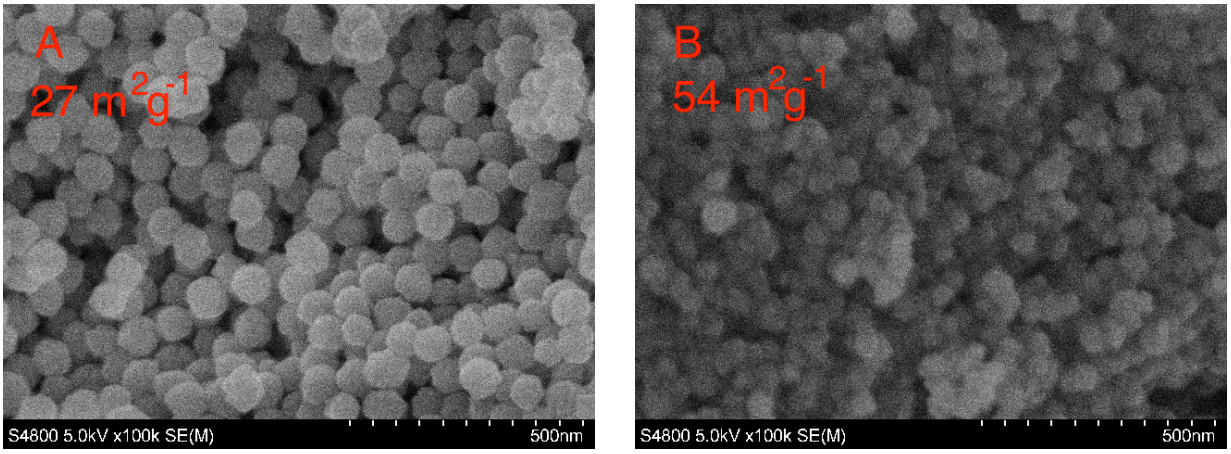

Figure 2: SEM images of synthesized hematite

A) Hematite synthesized following the method of Pedersen et al. (2005) B) Hematite synthesized according to Method 2 Iron Oxides in the Laboratory (Schwertmann & Cornell, 2000).

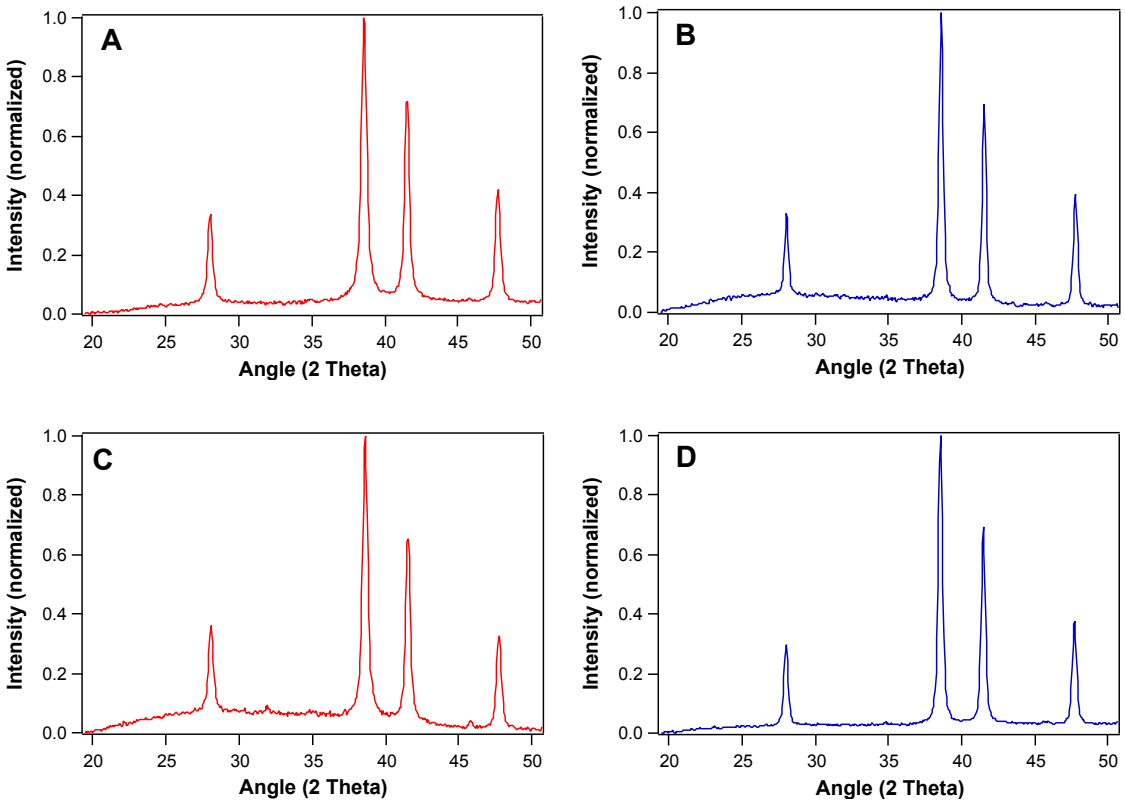

Figure 3: XRD spectra for unreacted and reacted hematite particles

A) Unreacted 54 m^2g^{-1} hematite. B) Unreacted 27 m^2g^{-1} hematite. C) 54 m^2g^{-1} hematite after 31-day isotope exchange reaction. D) 27 m^2g^{-1} hematite after 30-day isotope exchange reaction.

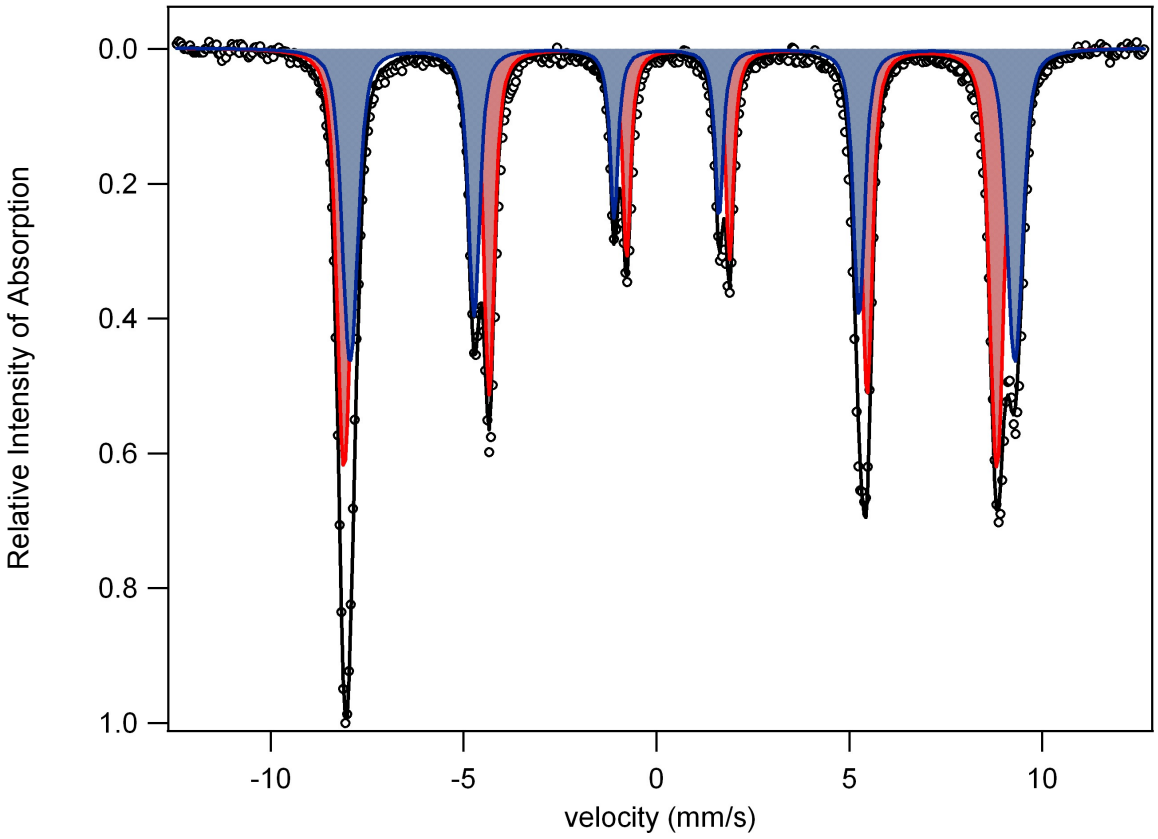

Figure 4: Mössbauer spectrum for unreacted 54 m^2g^{-1} hematite particles.

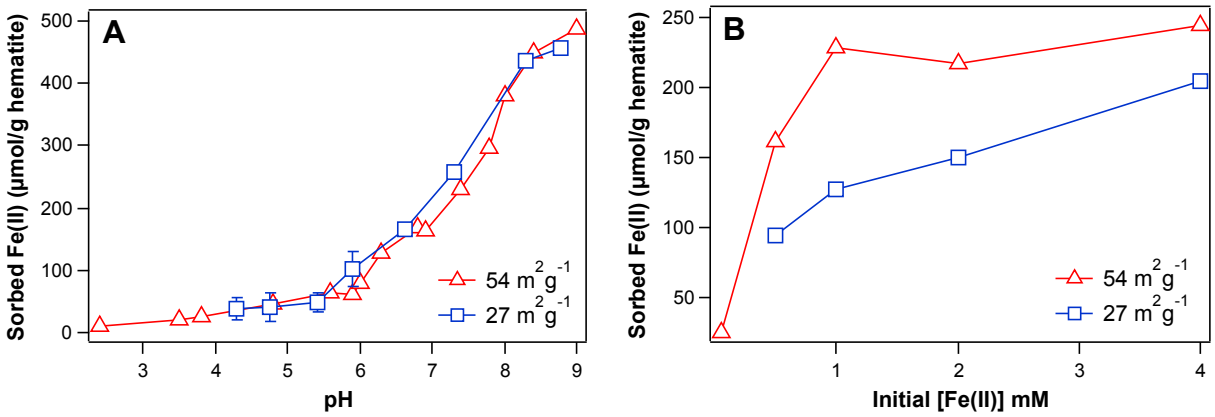

Figure 5: Sorption of Fe(II) on hematite

A) pH edges on 2 g/L hematite with 1 mM aqueous Fe(II). B) Sorption isotherm on 54 m^2g^{-1} and 27 m^2g^{-1} hematite with 2.0 g/L hematite at pH 7.5.

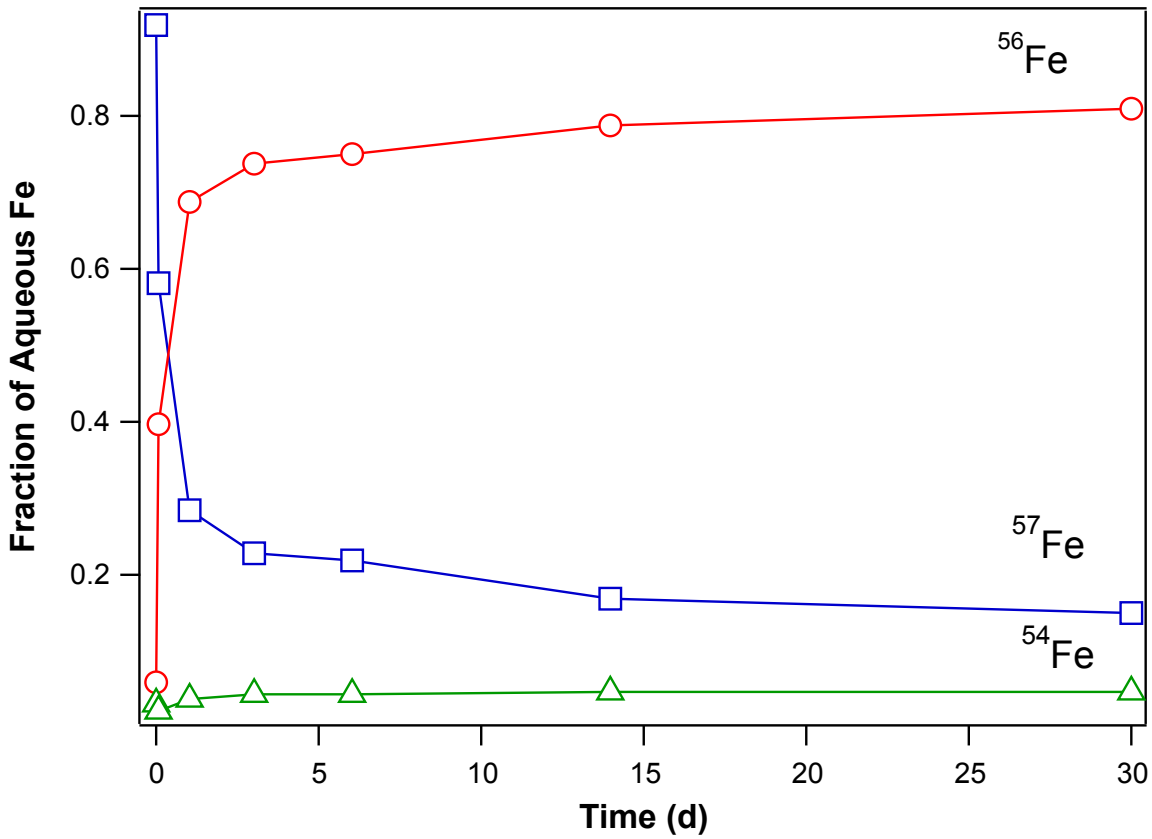

Figure 6: Isotope composition of aqueous Fe(II) over time

Aqueous Fe(II) isotope fractions over time during reaction with 54 m^2g^{-1} hematite at pH 7.0. Aqueous Fe(II) was initially enriched in ^{57}Fe, while the hematite contained iron at natural isotopic abundance.

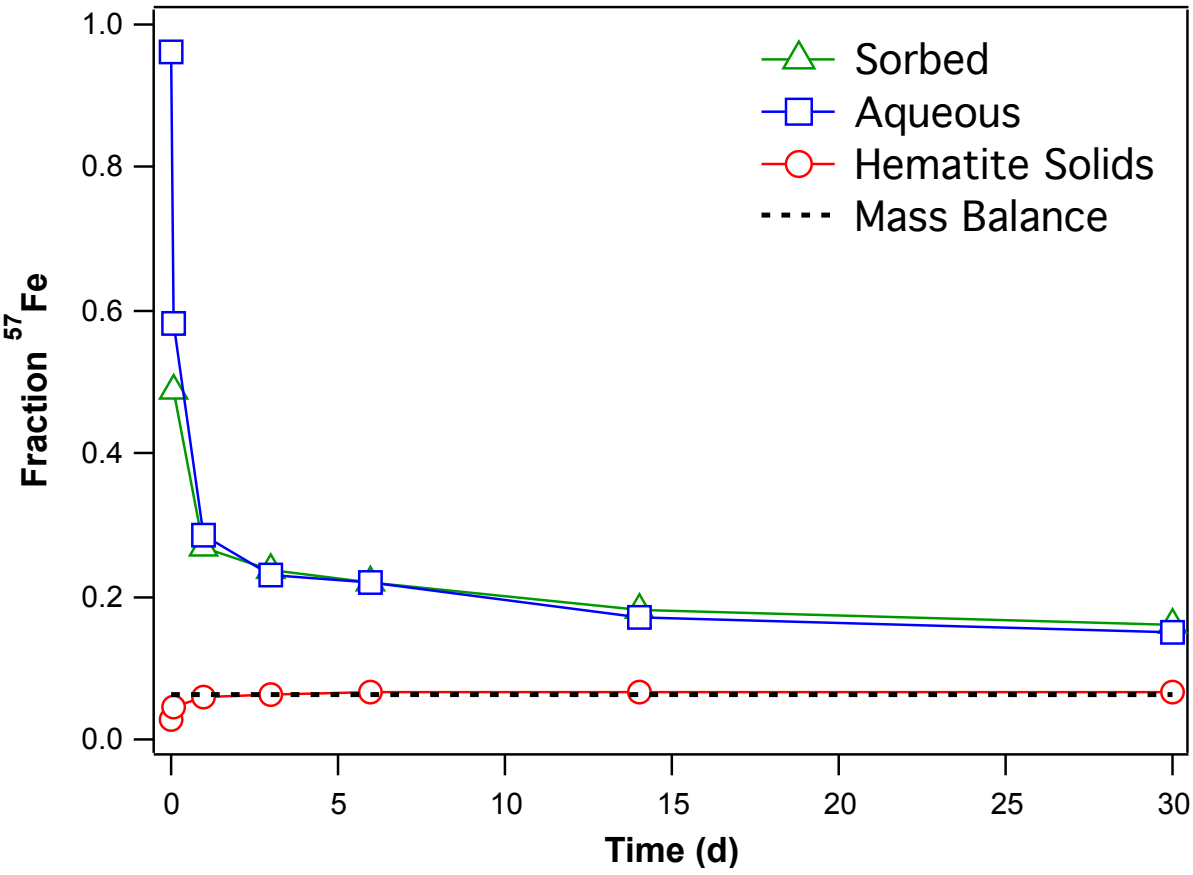

Figure 7: Fractions of ^{57}Fe in each reaction phase over time

^{57}Fe fractions in aqueous, solid, and sorbed phases over time during reaction between 54 m^2g^{-1} hematite and 1.0 mM $^{57}Fe(II)$ (2 g/L solids loading, pH 7.0). A mass balance line is included for reference.

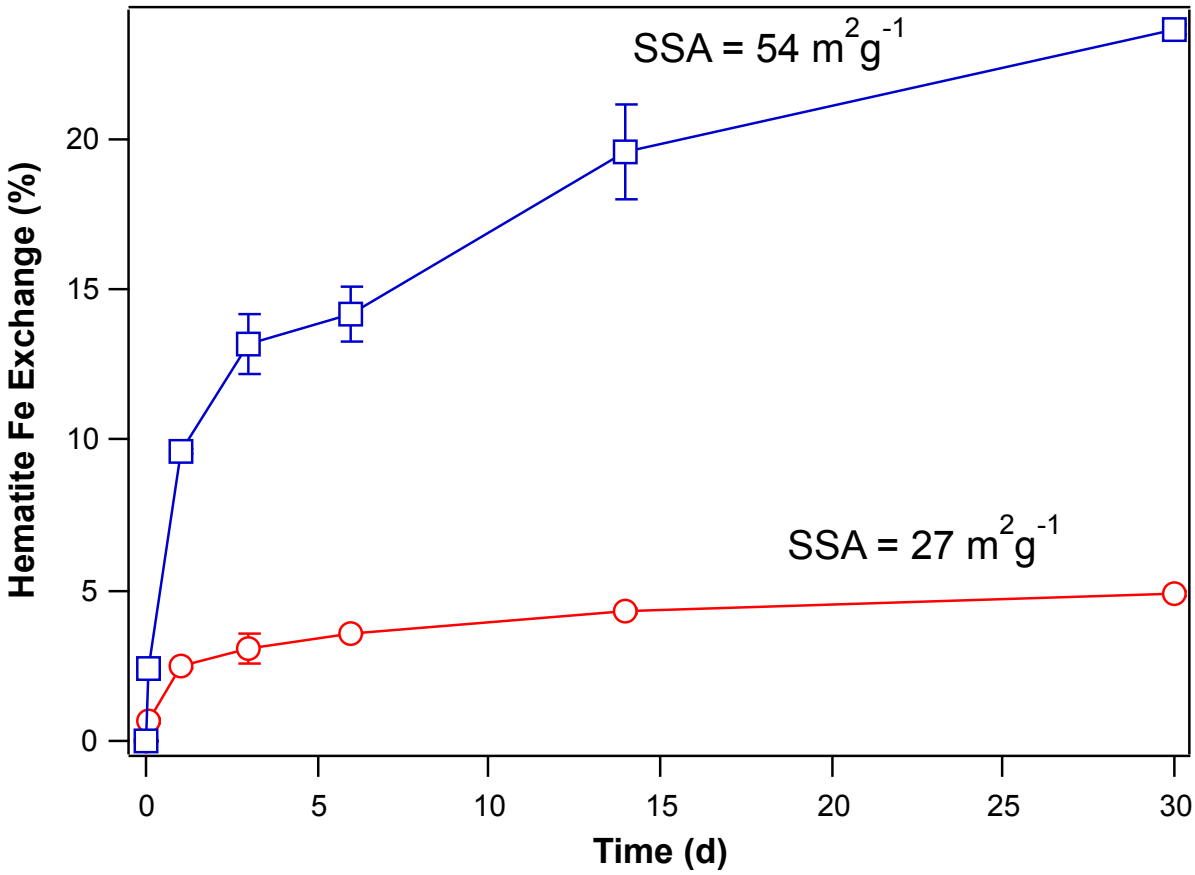

Figure 8: Percent exchange of Fe with varying particle size

Percent exchange of Fe in hematite over time for 27 m^2g^{-1} and 54 m^2g^{-1} hematite. Exchange reactions were carried out at pH 7.5 with an initial Fe(II) concentration of 1.0 mM and a solids loading of 2 g/L.

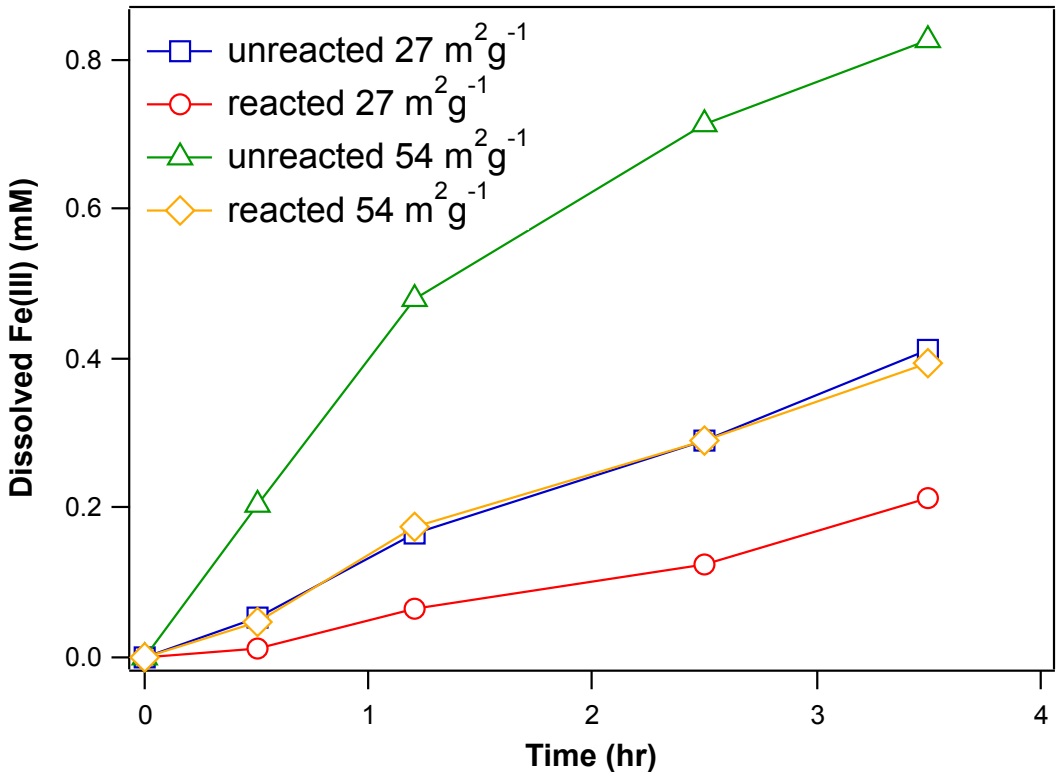

Figure 9: Acid dissolution of reacted and unreacted hematite particles.

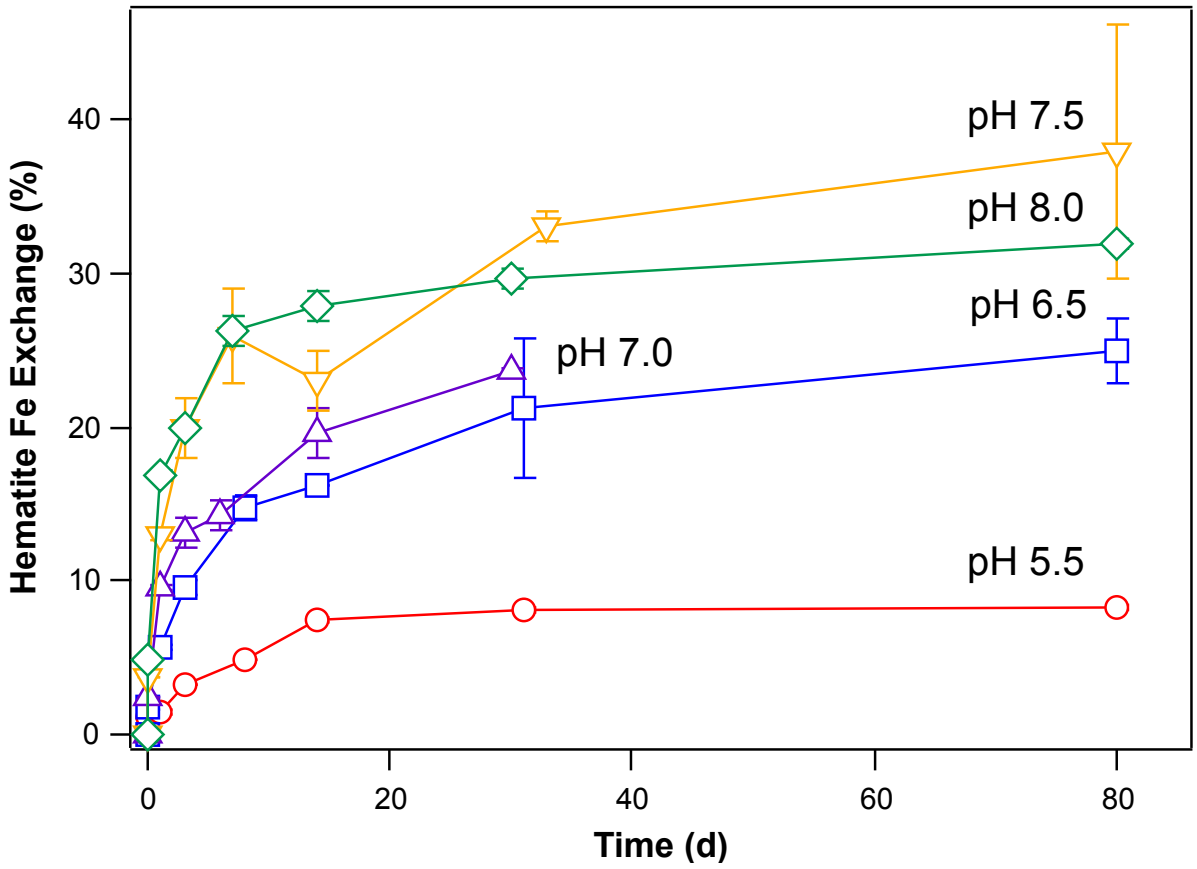

Figure 10: Percent exchange of Fe with varying pH

Percent exchange over time using 54 m^2g^{-1} hematite at different pH values. Exchange reactions were carried out with an initial Fe(II) concentration of 1.0 mM and a solids loading of 2 g/L.

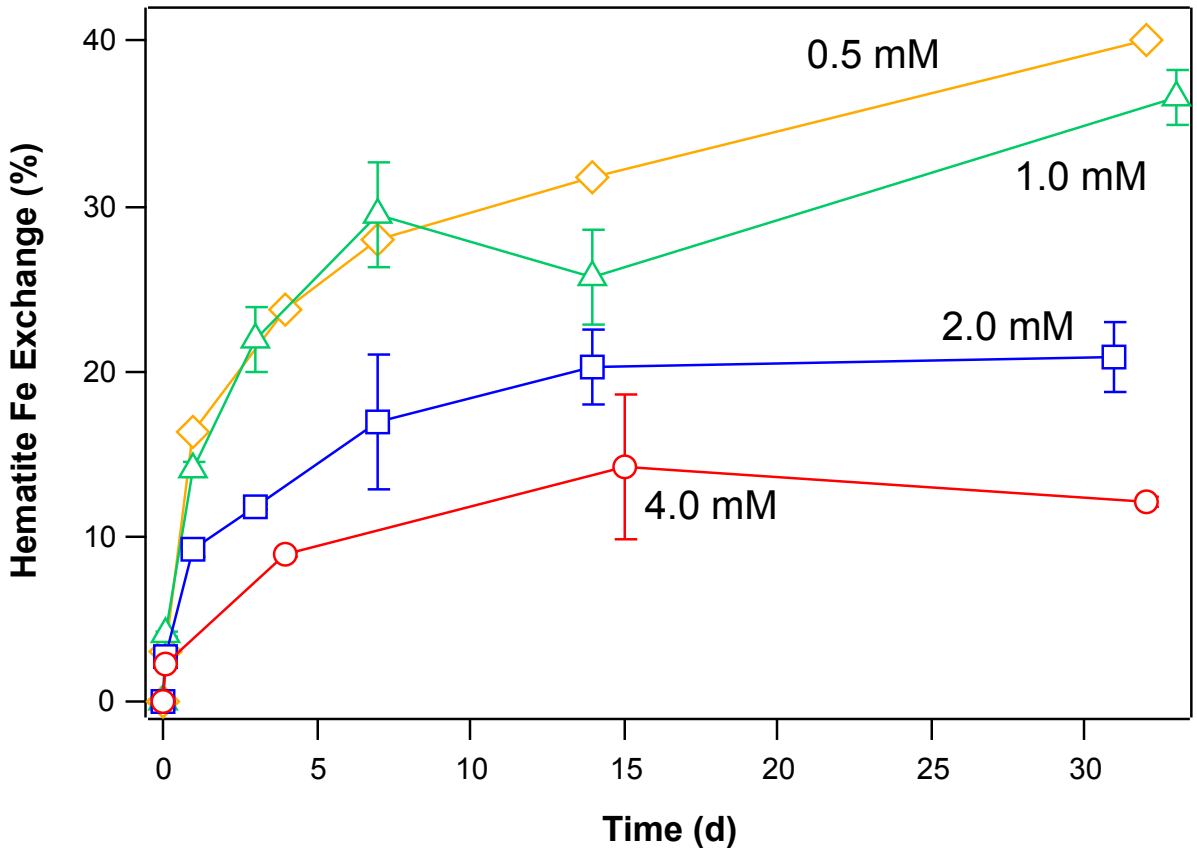

Figure 11: Percent exchange of Fe with varying Fe(II) concentration

Percent exchange over time using 54 m^2g^{-1} hematite at varying initial concentrations of Fe(II). Exchange reactions were carried out at pH 7.5 with a solids loading of 2 g/L.

REFERENCES

Boland, D., Collins, R., Miller, C., Glover. C & Waite, D. (2014). Effect of solution and solid-phase conditions on the Fe(II)-accelerated transformation of ferrihydrite to lepidocrocite and goethite. *Environmental Science and Technology, 48*, 5477 – 5485.

Boland, D., Collins, R., & Glover, C. (2014). Reduction of U(VI) by Fe(II) during the Fe(II)-accelerated transformation of ferrihydrite. *Environmental Science and Technology, 48,* 9086 – 9093.

Bora, D., Braun, A., & Constable, C. (2013). "In rust we trust." Hematite – the prospective inorganic backbone for artificial photosynthesis. *Energy and Environmental Science, 6*, 407 – 425.

Bose, S., Hochella, M., Gorby, Y., Kennedy, D., McCready, D., Madden, A. & Lower, B. (2009). Bioreduction of hematite nanoparticles by the dissimilatory iron reducing bacterium *Shewanella oneidensis* MR-1. *Geochimica et Cosmochimica Acta, 73,* 962 – 976.

Cwiertny, D., Handler, R., Schaefer, M. Grassian, V. & Scherer, M. (2008). Interpreting nanoscale size-effects in aggregated Fe-oxide suspensions: reaction of Fe(II) with goethite. *Geochimica et Cosmochimica Acta, 72*, 1365 – 1380.

Echigo, T., Monsegue, N., Aruguete, D., Murayama, M. & Hochella, M. (2013). Nanopores in hematite (α-Fe_2O_3) nanocrystals observed by electron tomography. *American Mineralogist, 98*, 154 – 162.

Frierdich, A., Luo, Y. & Catalano, J. (2011). Trace element cycling through iron oxide minerals during redox-driven dynamic recrystallization. *Geology, 39*, 1083 – 1086.

Frierdich, A. & Catalano, J. (2012). Fe(II)-mediated reduction and repartitioning of structurally incorporated Cu, Co, and Mn in iron oxides. *Environmental Science and Technology, 46*, 11070 – 11077.

Frierdich, A., Beard, B., Reddy, T., Scherer, M. & Johnson, C. (2014). Iron isotope fractionation between aqueous Fe(II) and goethite revisited: New insights on a multi-direction approach to equilibrium and isotopic exchange rate modification. *Geochimica et Cosmochimica Acta, 139*, 383 – 398.

Gorski, C., Handler, R., Beard, B., Pasakarnis, T., Johnson, C. & Scherer, M. (2012). Fe atom exchange between aqueous Fe2+ and magnetite. *Environmental Science and Technology, 46*, 12399 – 12407.

Guo, H., Xu, H., & Barnard, A. (2013). Can hematite nanoparticles be an environmental indicator? *Energy and Environmental Science, 6*, 561 – 569.

Handler, R., Beard, B., Johnson, C. & Scherer, M. (2009). Atom exchange between aqueous Fe(II) and goethite: an Fe isotope tracer study. *Environmental Science and Technology, 43*, 1102 – 1107.

Handler, R., Frierdich, A., Johnson, C., Rosso, M., Beard, B., Wang, C., Latta, D., Neumann, A., Pasakarnis, T., Premaratne, W. & Scherer, M. (2014). Fe(II)-catalyzed recrystallization of goethite revisited. *Environmental Science and Technology, 48*, 11302 – 11311.

Jeon, B., Dempsey, B., Burgos, W., Royer, R. & Roden, E. (2004). Modeling the sorption kinetics of divalent metal ions to hematite. *Water Research, 38*, 2499 – 2504.

Jones, A., Collins, R., Rose, J. & Waite, T. (2009). The effect of silica and natural organic matter on the Fe(II)-catalysed transformation and reactivity of Fe(III) minerals. *Geochimica et Cosmochimica Acta, 73*, 4409 – 4422.

Kappler, A., Amstaetter, K, & Borch, T. (2011). Arsenic redox transformation by humic substances and Fe minerals. *Applied Geochemistry, 26*, S317.

Latta, D., Bachman, J. & Scherer, M. (2012). Fe electron transfer and atom exchange in goethite: influence of Al-substitution and anion sorption. *Environmental Science and Technology, 46*, 10614 – 10623.

Larese-Casanova, P. & Scherer, M. (2007). Fe(II) sorption on hematite: new insights based on spectroscopic measurements. *Environmental Science and Technology, 41*, 471 – 477.

Larese-Casanova, P. & Scherer, M. (2007). Morin transition suppression in polycrystalline (57)hematite (alpha-Fe2O3) exposed to Fe-56(II). *Hyperfine Interactions, 174*, 111-119.

Larese-Casanova, P., Kappler, A., & Haderlein, S. (2012). Heterogenous oxidation of Fe(II) on iron oxides in aqueous systems: Identification and controls of Fe(III) product formation. *Geochimica Et Cosmochimica Acta, 91*, 171 -186.

Pedersen, H., Postma, D., Jakobsen, R. & Larsen, O. (2005). Fast transformation of iron oxyhydroxides by the catalytic action of aqueous Fe(II). *Geochimica et Cosmochimica Acta, 69*, 3967 – 3977.

Piepenbrock, A., Schroder, C. & Kappler, A. (2014). Electron transfer from humic substances to biogenic and abiogenic Fe(III) oxyhydroxide minerals. *Environmental Science and Technology, 48*, 1656 – 1664.

Schwertmann, U., & Cornell, R. (2000). *Iron Oxides in the Laboratory* (2nd ed.). Weinheim: WILEY-VCH.

Williams, A. & Scherer, M. (2004). Spectroscopic evidence for Fe(II)-Fe(III) electron transfer at the iron oxide-water interface. *Environmental Science and Technology, 38*, 4782 – 4790.

Yanina, S. & Rosso, K. (2008). Linked reactivity at mineral-water interfaces through bulk crystal conduction. *Science, 320*, 218 – 220.